

Silver(I) coordination polymers based on nitrile-functionalized mixed-donor ligands of different flexibility

Alexander J. Blake^{a,*}, Carla M. Aragoni^b, Massimiliano Arca^b, Claudia Caltagirone^b, Alessandra Garau^b, Vito Lippolis^{b,*}, Giacomo Picci^b, Enrico Podda^c, Riccardo Montis^d

^a School of Chemistry, University of Nottingham, University Park, Nottingham NG7 2RD, UK

^b Dipartimento di Scienze Chimiche e Geologiche, Università degli Studi di Cagliari, S.S. 554 Bivio per Sestu, 09042 Monserrato (CA), Italy

^c Centro Servizi di Ateneo per la Ricerca-CeSAR, Università degli Studi di Cagliari, 09042 Monserrato (CA), Italy

^d Dipartimento di Scienze Pure e Applicate, Università degli Studi di Urbino "Carlo Bo", Via Aurelio Saffi, 2-61029 Urbino, PU, Italy

ARTICLE INFO

Keywords:

Silver(I)

Macrocycles

Nitrile group

Coordination polymer

ABSTRACT

The nitrile-functionalized derivatives of 2,8-dithia-5-aza-2,6-pyridinophane ([12]anePyNS₂) (Py = Pyridine), 1-aza-4,7,10-trithiacyclododecane ([12]aneNS₃), and *N,N'*-bis(2-pyridylmethyl)-propylenediamine (Pypn), referred to as **L**¹⁰, **L**¹¹ and **L**¹², respectively, have been prepared. Following the reaction of these ligands with silver(I) salts, the three coordination polymers (CPs) {[Ag(**L**¹⁰)](BF₄)_∞}, {[Ag(**L**¹¹)](BF₄)•½MeCN}_∞, and {[Ag(**L**¹²)](NO₃)_∞}, have been isolated and structurally characterized. The structural features of the three CPs depends more on the nature of the un-functionalized ligands rather than on the presence of the nitrile groups. A comparative analysis of the structures of the three CPs is performed in relation to the structures of polymeric silver(I) compounds obtained with nitrile-functionalized pendant arms of related aza- and mixed donor macrocyclic ligands (**L**¹–**L**⁹) reported in the literature.

1. Introduction

During the past quarter century, the inorganic crystal engineering of coordination polymers (CPs) and metal organic frameworks (MOFs) has experienced an exponential growth resulting in the development of innovative solid functional materials for applications in microelectronics, nonlinear optics, gas storage, molecular sensing, ion exchange, and drug-delivery [1–7]. In the late 1990s, most of the efforts were devoted to the targeted construction of new architectures and networks of desired topologies in the solid state (from molecular interlocked/intertwined species such as rotaxanes, catenanes, knots and helicates, to molecular rings and cages, and extended 1D, 2D and 3D networks) by exploiting the self-assembly of organic ligands with appropriate functional groups and metal ions, making use, in the first place, of the strength and directionality of coordination bonds [8].

Many advances have been made with the aim of allowing predictable control over the topology of the supramolecular architectures formed in the solid state, through a careful choice of the organic (spacers) and inorganic (metal ions or coordinatively unsaturated preformed complexes) building-blocks. However, this objective is still a major

challenge due to the intervention of weaker interactions such as hydrogen or halogen bonds, π•••π interactions and other non-covalent contacts involving groups belonging to the organic or inorganic components of the coordination polymer, in determining the packing arrangement of the polymeric entities.

In 1998, in Martin Schroder's group, the idea came up to consider for the first time functionalized pendant arm derivatives of macrocyclic ligands for the purpose of constructing multidimensional inorganic polymers. In fact, until then aza- and mixed thia-aza macrocyclic ligands had been used extensively as ligands for the preparation of complexes of high kinetic inertness and thermodynamic stability, with pendant groups often attached to the macrocyclic framework in order to promote endocyclic complexation and to impart specific redox and coordination environments to the coordinated metal ions. It was argued that nitrile-containing pendant arms would promote the formation of multinuclear and multidimensional exocyclic solid state architectures with metal ions such as Ag^I and Cu^I, rather than endocyclic coordination and the formation of mononuclear complexes, due to the inability of the nitrile group to bind *via* σ M←:N≡C–R donation in a chelate fashion to a metal ion sitting within the macrocyclic cavity. In the same period Ciani

* Corresponding authors.

E-mail addresses: alexanderjohnblake@outlook.com (A.J. Blake), lippolis@unica.it (V. Lippolis).

<https://doi.org/10.1016/j.ica.2023.121648>

Received 5 March 2023; Received in revised form 22 May 2023; Accepted 17 June 2023

Available online 19 June 2023

0020-1693/© 2023 The Authors. Published by Elsevier B.V. This is an open access article under the CC BY license (<http://creativecommons.org/licenses/by/4.0/>).

and coworkers obtained interesting coordination networks from the self-assembly of silver(I) salts and aliphatic linear chain dinitriles NC(CH₂)_nCN (n = 2–8, 10) [9–11], after a lot of evidence of silver(I) coordination polymers formed with aromatic nitrogen donor ligands [12].

The results achieved with the nitrile-functionalized pendant arm derivatives reported in Fig. 1 confirmed the active role of the nitrile groups in linking different silver(I) centers in the obtained polynuclear complexes with their dimensionality strictly dependent upon the number and length of nitrile-functionalized pendant arms present in the ligands (especially those featuring 9-membered macrocyclic rings), and the donor set and ring size of the macrocyclic framework [13,14].

Additional support for the initial working idea was provided by the reactivity of L⁵ and L⁶ with AgBF₄ in the presence of half an equivalent of CN⁻ or SCN⁻. In this case, the coordination site left free on the metal center by the macrocyclic moiety of the nitrile-functionalized ligands was occupied by the exogenous anionic ligands instead of nitrile groups, thus preventing the formation of inorganic polymers involving the pendant nitriles and favoring the isolation of unusual compounds, in particular discrete binuclear complexes featuring either a side-on two-electron (σ) μ₂-kC:kC or a linear four-electron (σ + π) μ₂-kC:kN bridging cyanide/thiocyanate [15–17].

Pursuing our interest in exploring the use of pendant arm derivatives of macrocyclic and pre-organized ligands as suitable building block for inorganic crystal engineering, we report on the compounds obtained by reacting silver(I) salts with the nitrile-functionalized mixed-donor ligands L¹⁰, L¹¹, and L¹² (Fig. 2) characterized by different degrees of flexibility and conformational freedom.

In particular, L¹¹, characterized by an NS₃-donor set in the 12-membered macrocyclic framework, is structurally analogous to L⁷. L¹⁰ features a pyridine subunit in the N₂S₂ donating 12-membered macrocyclic moiety, while L¹² is an open-chain and more flexible ligand

characterized by two pyridine subunits and two tertiary N-donors in the N₄ N,N'-bis(2-pyridylmethyl)-propylenediamine (Pypn) chelating unit (Fig. 2).

2. Results and discussion

L¹⁰ and L¹¹ were successfully synthesized by direct reaction, respectively, of the macrocycles 2,8-dithia-5-aza-2,6-pyridinophane ([12]anePyNS₂) (Py = Pyridine) and 1-aza-4,7,10-trithiacyclododecane ([12]aneNS₃) with acrylonitrile, and used as precursors in the synthesis of the corresponding amino derivatives for the development of fluorescent chemosensors for heavy metal ions [18,19]. However, their coordination chemistry has not been considered to date. The X-ray crystal structure of L¹⁰ (see Fig. S1 and Tables S1 and S2 in Supporting Information, SI) shows the aliphatic portion of the macrocyclic framework folded over the pyridine unit. The S-donors and the aliphatic N-donor are *exo*-oriented with the S–C–N torsion angles assuming an *anti*-arrangement, while the torsion angles at the C–S and C–N (aliphatic) bonds assume *gauche*-arrangements. A similar conformation was observed for the compound 5-(dansylamidopropyl)-2,8-dithia-5-aza-2,6-pyridinophane [18].

L¹⁰ was treated with AgBF₄ in a 1:1 molar ratio in MeCN (the choice of AgBF₄ as starting silver(I) salt was determined by the necessity to limit the effect of the counter-anion and to compare the results with those obtained with the nitrile-functionalized pendant arm derivatives in Fig. 1 for which this silver(I) salt was mainly considered). Although analytical and mass spectrometric data for the product are consistent with a 1:1 [Ag(L¹⁰)]BF₄ stoichiometry, the single crystal structure determination (Table S1) reveals the formation of the polymeric compound {[Ag(L¹⁰)](BF₄)_∞} where, contrary to what was expected, the nitrile group in L¹⁰ is not involved in metal coordination. Each Ag^I ion is

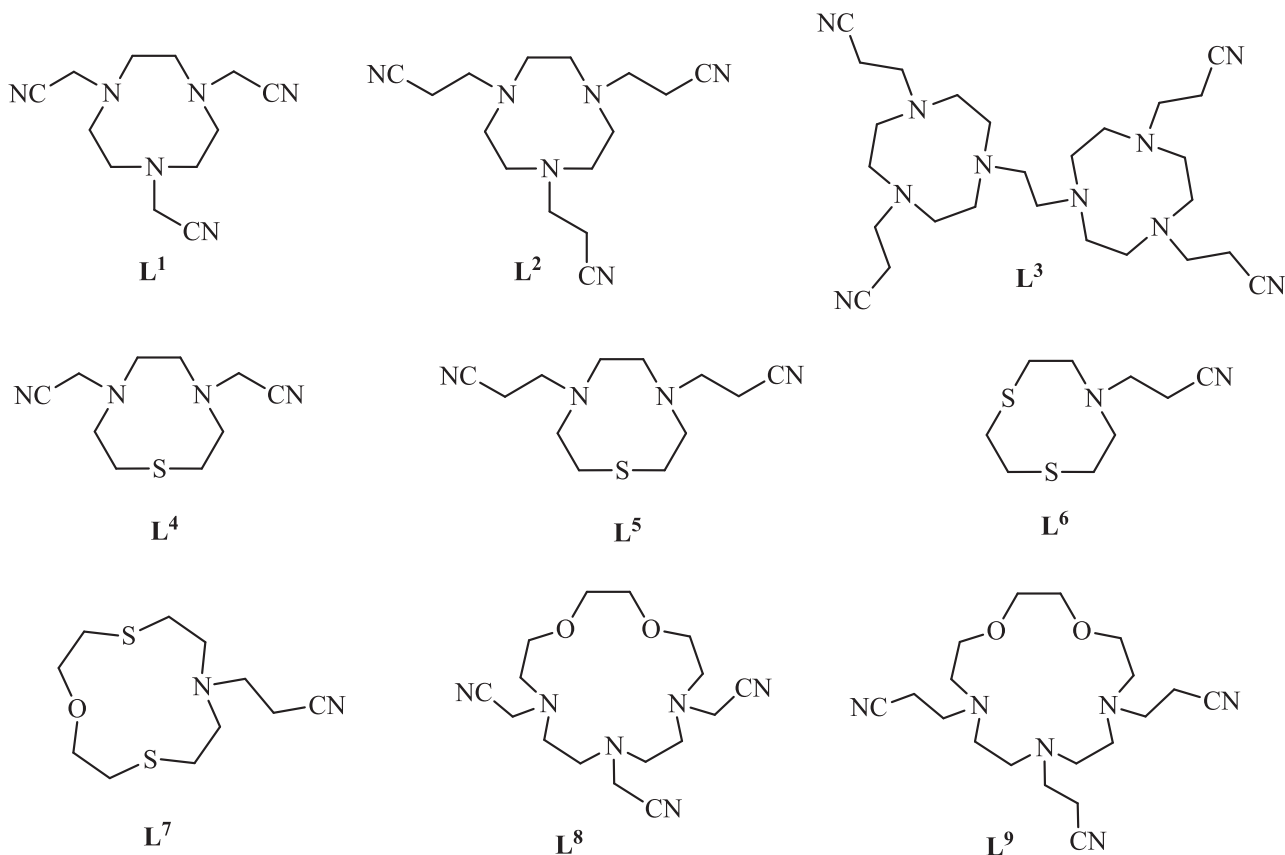


Fig. 1. Nitrile-functionalized derivatives of macrocyclic ligands considered in previous studies for the construction of silver(I) inorganic polymers of different dimensionality [13,14].

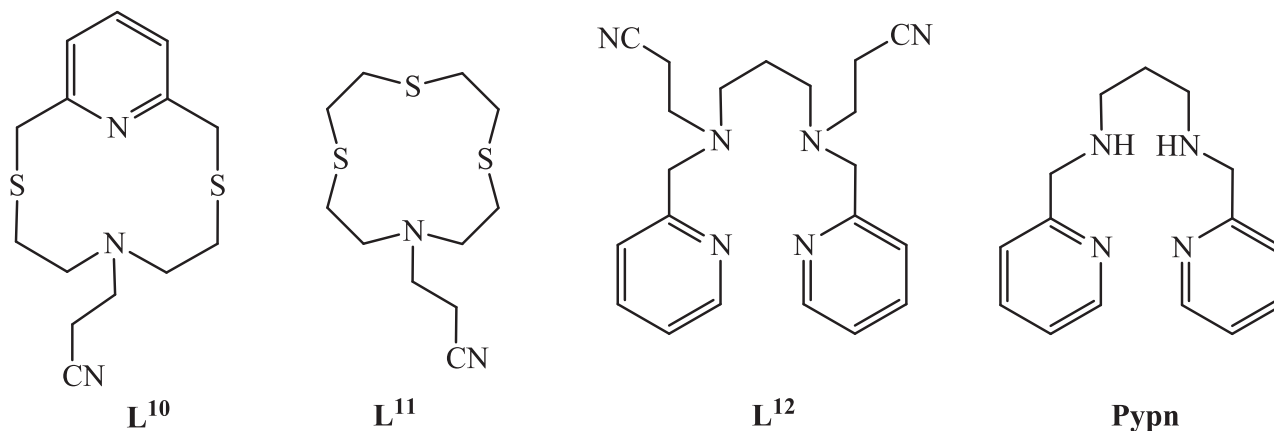


Fig. 2. Nitrile-functionalized mixed-donor ligands considered in this paper.

bound to the two S atoms (S1 and S2) [Ag1–S1 = 2.7415(6), Ag1–S2 = 2.5830(7) Å], the pyridine N atom (N1) [Ag1–N1 = 2.419(2) Å], and the tertiary N atom (N2) [Ag1–N2 = 2.652(2) Å] from the macrocyclic unit. An overall distorted square pyramidal coordination geometry is completed by the sulfur atom, S1ⁱ, of a symmetry-related [Ag(L¹⁰)]⁺ unit [Ag1–S1ⁱ = 2.5237(6) Å, symmetry code $i = 3/2 - x, 1/2 + y, 1/2 - z$] (Fig. 3).

Interestingly, the distances between the metal center and both the aliphatic N-donor (N2), in *trans*-position to the pyridine moiety, and the S1 atom are longer than those generally observed for Ag–N and Ag–S covalent bonds in silver(I) complexes with aza- and mixed thia-aza macrocycles [14,20]. Furthermore, the intermolecular Ag1–S1ⁱ bond distance is significantly shorter than the intramolecular Ag1–S1 one, with a S1–Ag1–S1ⁱ angle of 98.5° (Fig. 3).

This *endo*- and *exo*-binding mode of S1 generates {[Ag(L¹⁰)]⁺}_∞ one-dimensional zig-zag coordination polymers running along the [010] direction, with the uncoordinated nitrile pendant arms alternately

located above and below the plane containing the –Ag–S–Ag–S– backbone chain, and the ligand adopting an overall $\mu_2\text{-}\kappa^1\text{N1}:\kappa^1\text{N2}:\kappa^2\text{S1}:\kappa^1\text{S2}$ binding mode. A similar polymeric structure was observed in the silver (I) complexes [Ag(L)](CF₃CO₂)•H₂O and [Ag(L)]NO₃ [21,22] in which L is the macrocycle 2,5,8-trithia-2,6-pyridinophane ([12]anePyS₃), which is structurally analogous to [12]anePyNS₂ but has an S-donor instead of the secondary amine nitrogen. However, in these silver (I) complexes, the bridging S atom is the central one in the thioether portion of the macrocyclic ligand, rather than one of the two next to the pyridine moiety.

The crystal packing features BF₄[−] anions that are intercalated between {[Ag(L¹⁰)]⁺}_∞ cationic zig-zag polymeric chains as shown in Fig. S2, weakly interacting via C–H•••F hydrogen bonds [the shortest C•••F distance is 3.121(3) Å].

Analogously to L¹⁰, L¹¹ has only one nitrile-functionalized pendant arm but the macrocyclic framework is characterized by a higher degree of flexibility due to the introduction of a sulfur atom in the donor set in

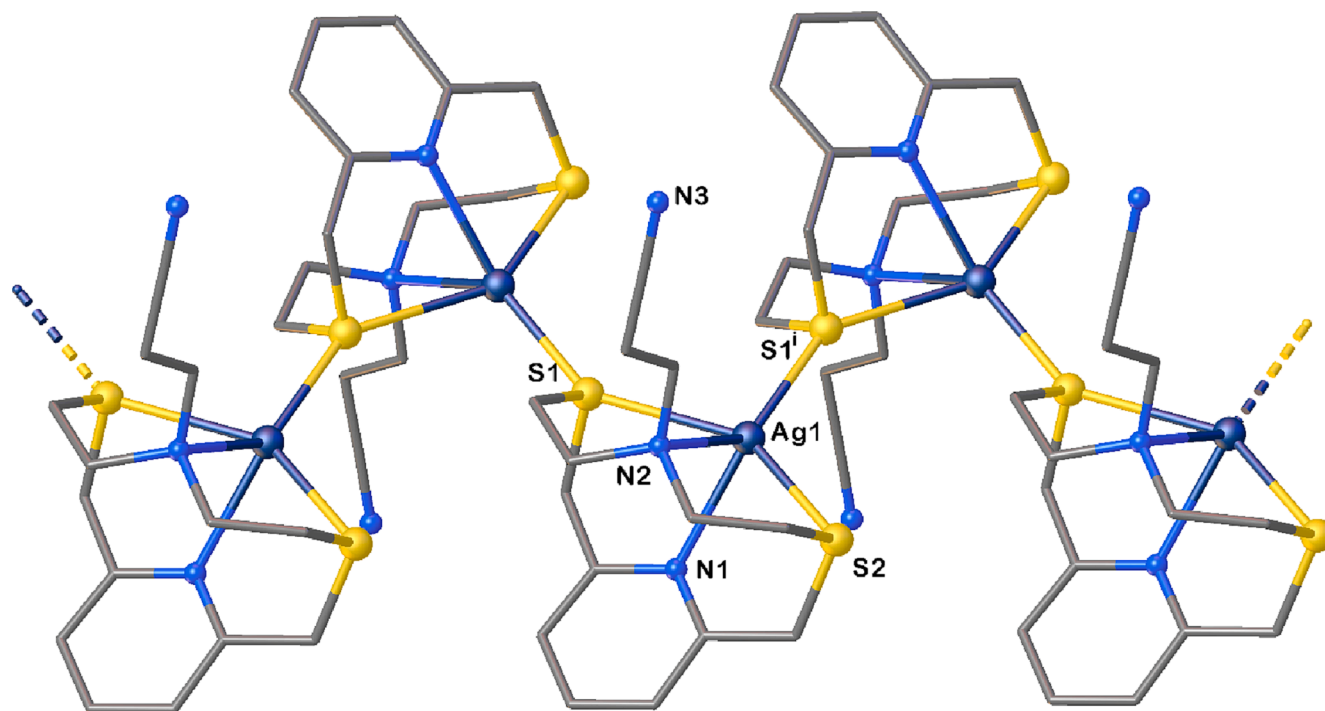


Fig. 3. A drawing showing part of a {[Ag(L¹⁰)]⁺}_∞ zig-zag polymeric chain in {[Ag(L¹⁰)](BF₄)_∞ running along the [010] direction with the numbering scheme adopted. Hydrogen atoms and counter anions are omitted for clarity [symmetry code $i = 3/2 - x, 1/2 + y, 1/2 - z$]. Selected bond length (Å) and angles (°) are reported in Table S3 in the SI.

place of the pyridine moiety. A four-coordinated quasi-tetrahedral structure around the Ag^{I} center might be achieved by the intervention of either the nitrile group from a second molecule of L^{11} as observed for L^{6} (Fig. 1) [14], or a sulfur atom from the macrocyclic moiety as observed for L^{10} , the [12]aneNS₃ moiety imposing, substantially, a NS₂ donation in both cases. As a matter of fact, reaction of L^{11} with AgBF_4 in a 1:1 molar ratio in MeCN afforded after crystallization colorless plate-shaped crystals (Table S1) corresponding to the formulation $[\text{Ag}(\text{L}^{\text{11}})]\text{BF}_4 \cdot \frac{1}{2}\text{MeCN}$, with the crystal structure featuring one-dimensional $\{[\text{Ag}(\text{L}^{\text{11}})]^+\}_\infty$ zig-zag polymeric chains (Fig. 4).

Each Ag^{I} center adopts a distorted tetrahedral geometry with the macrocyclic unit imposing a NS₂ tri-coordination [Ag1–N1 = 2.506(2), Ag1–S1 = 2.5602(7), Ag1–S3 = 2.5272(7) Å] and assuming a square shape with the donor atoms part of a “side”, each of which features a sequence of *gauche-anti-gauche* torsion angles. The fourth coordination site of the tetrahedral environment is occupied by the S2 atom from a symmetry-related $[\text{Ag}(\text{L}^{\text{11}})]^+$ complex cation [Ag1–S2ⁱ 2.5227(7) Å, symmetry code $i = 3/2 - x, -1/2 + y, +z$]. The intramolecular Ag1–S2 distance (green dashed lines in Fig. 4) is too long [3.192(7) Å] to be associated with an Ag–S covalent bond and to consider the overall coordination environment as distorted square-pyramidal. Furthermore, the intermolecular Ag1–S2ⁱ bond distance is shorter than the intramolecular ones. The *exo*-coordination of S2 generates one-dimensional zig-zag coordination polymers running along the [010] direction, with the uncoordinated nitrile pendant arms oriented alongside the propagation direction of the –Ag–S•••Ag–S••• backbone chain. Similarly to the crystal structure of $\{[\text{Ag}(\text{L}^{\text{10}})](\text{BF}_4)\}_\infty$, in $\{[\text{Ag}(\text{L}^{\text{11}})](\text{BF}_4) \cdot \frac{1}{2}\text{MeCN}\}_\infty$, BF_4^- anions are also intercalated among cationic zig-zag polymeric chains weakly interacting via C–H•••F hydrogen bonds [the shortest C•••F distance is 3.146(4) Å]. Furthermore, co-crystallized acetonitrile molecules lie on a two-fold screw axis as shown in the packing diagrams depicted in Fig. S3.

In view of the different S atoms participating in the intermolecular Ag–S bond, the polymeric cationic $\{[\text{Ag}(\text{L}^{\text{11}})]^+\}_\infty$ chains resemble more those observed in $[\text{Ag}(\text{L})](\text{CF}_3\text{CO}_2) \cdot \text{H}_2\text{O}$ and $[\text{Ag}(\text{L})]\text{NO}_3$ [21,22] [$\text{L} = 2,5,8$ -trithia-2,6-pyridinophane ([12]anePyNS₃)], than the zig-zag $\{[\text{Ag}(\text{L}^{\text{10}})]^+\}_\infty$ polymers, with L^{11} adopting an overall $\mu_2\text{-}\kappa^1\text{N1}:\kappa^1\text{S1}:\kappa^1\text{S2}:\kappa^1\text{S3}$ binding mode. Worthy of note, in the case of L^{7} (Fig. 1) [14], the discrete binuclear complex cation $[\text{Ag}_2(\text{L}^{\text{7}})_2]^{2+}$ was

formed upon reaction with AgBF_4 in a 1:1 molar ratio in MeCN, in which each metal center is coordinated by a [NS₂+O] donor set from the [12]aneNS₂O macrocyclic framework and the nitrile group of a symmetry-related $[\text{Ag}(\text{L}^{\text{7}})]^+$ unit in a distorted trigonal bipyramidal coordination sphere. Despite the soft character of the Ag^{I} metal ion, the quite short and unpredictable Ag–O distance [2.788(6) Å] in $[\text{Ag}_2(\text{L}^{\text{7}})_2]^{2+}$ as compared to the quite long intermolecular Ag–S one in $\{[\text{Ag}(\text{L}^{\text{11}})]^+\}_\infty$, together with packing solid state effects, might be responsible for the different coordination behavior of the two analogous L^{7} and L^{11} ligands. Interestingly, dimetallo[3.3]para- and metacyclophanes were obtained from the reaction of pyridylmethyl-armed [12]aneNS₃ with silver triflate (AgOTf) [23]. Therefore, L^{10} and L^{11} featuring NS₃-donating 12-membered macrocyclic units, do not afford multidimensional coordination polymers with silver(I) thanks to the intervention of the nitrile groups as observed for the nitrile-functionalized derivatives of 9-membered macrocycles $\text{L}^{\text{1}}\text{--}\text{L}^{\text{3}}$, L^{5} , L^{6} (Fig. 1) [13,14]. The polymeric structures observed in the case of $\{[\text{Ag}(\text{L}^{\text{10}})](\text{BF}_4)\}_\infty$ and $\{[\text{Ag}(\text{L}^{\text{11}})](\text{BF}_4) \cdot \frac{1}{2}\text{MeCN}\}_\infty$ are instead determined by the bridging action of a sulfur atom belonging to the macrocyclic unit. This behavior appears to be a recurring feature in the chemistry of pendant arm derivatives of [12]aneNS₃ with silver(I). In fact, Habata and coworkers reported a series of ligands featuring [12]aneNS₃ bearing aromatic side arms, with either electron-donating groups (EDGs) or electron-withdrawing groups (EWGs) as substituents on the phenyl ring. The structures of the corresponding silver(I) complexes were determined by the intermolecular CH•••π interactions controlled by the nature of the substituents EDGs or EWGs on the aromatic side arms, being CPs or trimers, respectively. In any case, the NS₃ coordination imposed by the macrocyclic unit to each metal center is completed by a sulfur atom from a neighboring complex unit in an overall penta-coordination [24]. A similar behavior was observed by Schröder and coworkers for the heteroditopic ligands [12]aneS₃N-CH₂CONH-^tBu and [12]aneS₃N-CH₂CONH(CO)NH-^tBu for metal salts: in the structure of the corresponding silver(I) coordination polymers, the pendant arms were engaged in binding the counter-anion of the starting silver(I) salt [25,26].

Polypyridyl ligands continue to be intensively studied in supramolecular chemistry because they have many degrees of freedom and few conformational constraints [27]. In particular *N,N'*-bis(2-pyridylmethyl)-propylenediamine (Pypn, Fig. 2), featuring four *N*-donors

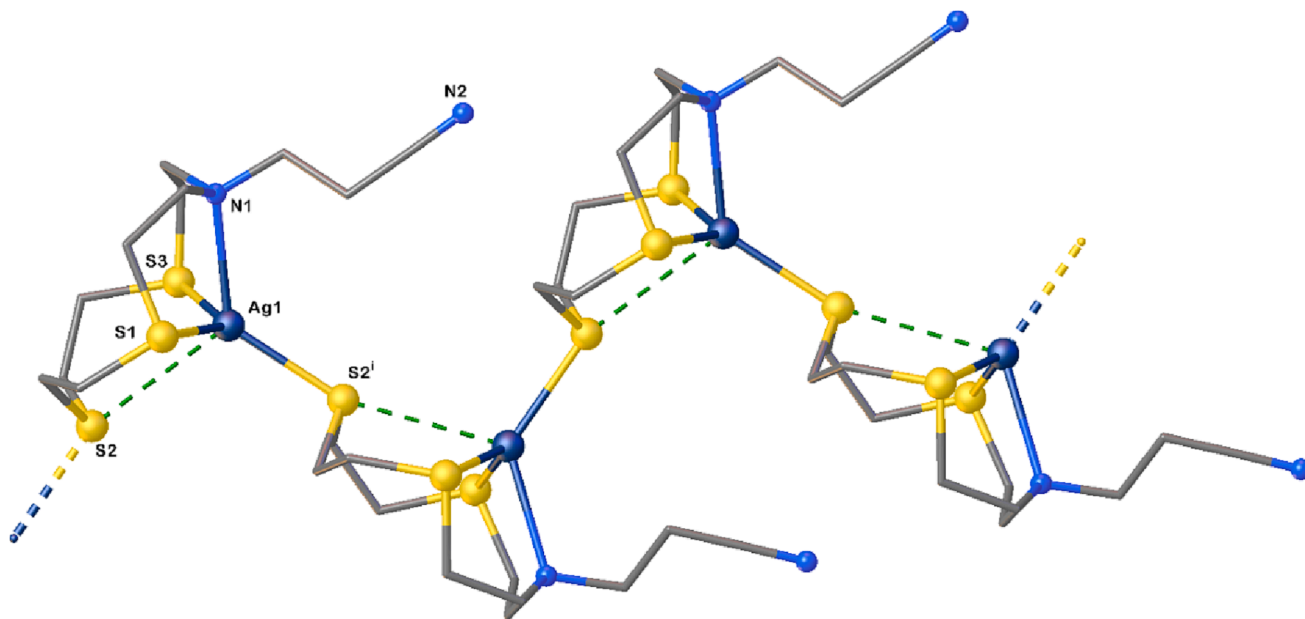


Fig. 4. A drawing showing part of a $\{[\text{Ag}(\text{L}^{\text{11}})]^+\}_\infty$ zig-zag polymeric chain in $\{[\text{Ag}(\text{L}^{\text{11}})](\text{BF}_4) \cdot \frac{1}{2}\text{MeCN}\}_\infty$ running along the [010] direction with the numbering scheme adopted. Hydrogen atoms and counter anions are omitted for clarity [symmetry code $i = 3/2 - x, -1/2 + y, +z$]. Selected bond lengths (Å) and angles (°) are reported in Table S4 in the SI.

for coordination in a chelating fashion, has been used to synthesize a number of either mononuclear or polynuclear transition-metal compounds in different coordination geometries and oxidation states [28–34]. Functionalization of the secondary N atoms for supramolecular functions [35,36], with pendant arms bearing nitrile groups has never been considered so far and, therefore, we reacted Pypn with acrylonitrile to afford L^{12} and to study its reactivity towards silver(I). Reaction of L^{12} with $AgNO_3$ in a 1:1 molar ratio in MeCN afforded colorless needle-shaped crystals upon recrystallization (Table S1) corresponding to the formulation $[Ag(L^{12})]NO_3$. Single-crystal X-ray diffraction analysis confirmed the formation of a 2D coordination polymer.

Each silver(I) center is bound to two pairs of N atoms, one pyridyl and one aliphatic, from two different L^{12} ligand units [$Ag1-N1 = 2.537(5)$, $Ag1-N3 = 2.227(5)$, $Ag1-N2^i = 2.700(5)$, $Ag1-N4^i = 2.214(5)$ Å; symmetry code $i = -1 + x, +y, +z$] with the two pyridyl ligands rotated by about 86° , to generate chains running along the [100] direction (see Fig. 5). Parallel polymeric chains of this kind are connected via $Ag1-N5^{ii}$ bonds of 2.717(7) Å (symmetry code $ii = +x, +y, -1 + z$) involving one nitrile pendant arm from an additional L^{12} ligand, thus completing the coordination sphere of the metal center into an overall very distorted trigonal bipyramidal N_5 environment. Therefore, each ligand unit adopts a $\mu_3-\kappa^1N1:\kappa^1N2:\kappa^1N3:\kappa^1N4:\kappa^1N5$ bridging mode involving one nitrile-functionalized pendant arm, while the second nitrile group is left uncoordinated, and each metal center can be regarded as a three-connected node, resulting in a 2D coordination polymer of fused 22-membered $Ag_3N_7C_{12}$ metallacycles lying in the (101) plane (Fig. 5a and S4) and a (6,3) net topology. The crystal packing features pairs of adjacent sheets that are staggered by about $c/2$ as shown in Fig. 5b. The NO_3^- anions are located in between the CPs layers forming bridging $C-H\cdots O$ hydrogen bonds [the shortest $C\cdots O$ distance is 3.145(9) Å] (Fig. S5).

Interestingly, when the unfunctionalized ligand Pypn was reacted with silver(I) perchlorate the formation of 1D helical polymeric chains was observed in the resulting compound of formulation $[Ag(Pypn)]$

ClO_4^- , with the ligand adopting a $\mu_2-\kappa^1N1:\kappa^1N2:\kappa^1N3:\kappa^1N4$ bridging coordination mode and the metal centers featuring a tetrahedral N_4 coordination environment [37]. In this compound, adjacent and nearly parallel right- or left-handed helical chains interact via $\pi\cdots\pi$ interactions between pyridyl rings to form a layered structure. Therefore, the presence of nitrile pendant arms in L^{12} is responsible for the increased dimensionality of the coordination polymer observed in the crystal structure of $\{[Ag(L^{12})](NO_3)_2\}_\infty$. This is also supported by the fact that the reaction between Pypn and silver(I) nitrate produced a crystalline product with formula $[Ag_2(Pyppn)](NO_3)_2 \cdot 2H_2O$, in which the layered motif is determined by both the organic linker coordinating four metal centers and adopting a $\mu_4-\kappa^1N1:\kappa^1N2:\kappa^1N3:\kappa^1N4$ bridging mode, and the nitrate anions participating in bridging two silver(I) nodes featuring a N_2O_2 and N_2O environment, respectively, that are also directly connected through argentophilic interaction [37].

3. Conclusions

In previous papers we have introduced the possibility of using nitrile-functionalized pendant arm derivatives of mixed-donor macrocycles as building blocks for the construction of multidimensional coordination polymers with metal ions such as silver(I) [13,14]. The results obtained so far indicate that the nitrile groups play an active role in determining the formation of inorganic polymers especially with small tridentate macrocycles such as [9]ane N_3 (1,4,7-triazacyclononane), [9]ane N_2S (1,4-diaza-7-thiacyclononane) and [9]ane NS_2 (1-aza-4,7-dithiacyclononane) (L) (see Table 1). The dimensionality of the resulting coordination polymers appears to be dependent upon the number of the nitrile-functionalized pendant arms present in the ligand, upon their length and upon the donor set of the macrocyclic ligands [13,14]. However, the results obtained by reacting nitrile-functionalized pendant arm derivatives of tridentate small macrocycles with silver(I) in the presence of exogenous anionic ligands such as CN^- and SCN^- indicate that beside steric effects related to the pendant arms, electronic factors can also play

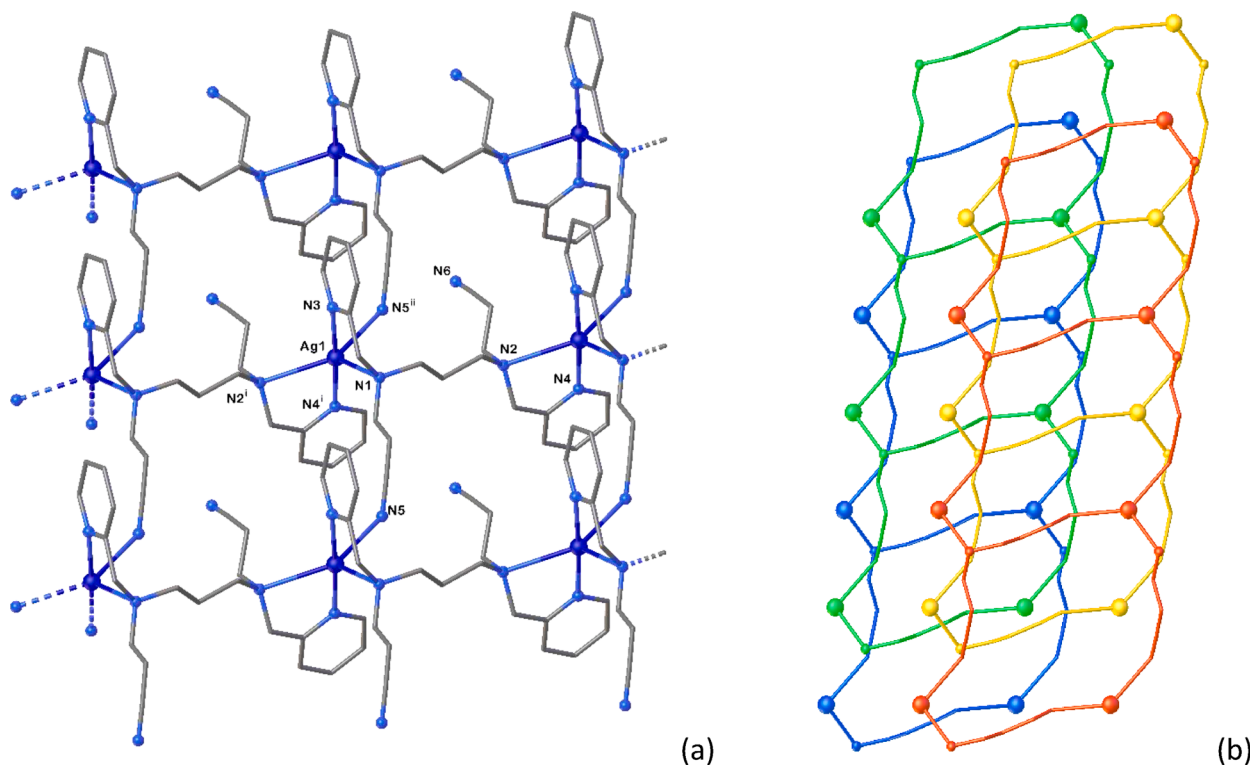
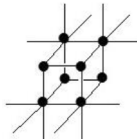

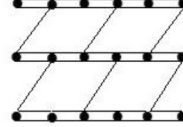






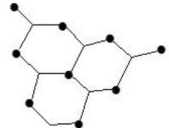


Fig. 5. A drawing viewed along the [010] direction showing (a) part of the $\{[Ag(L^{12})]^+\}_\infty$ 2D structure in $\{[Ag(L^{12})](NO_3)_2\}_\infty$ with the numbering scheme adopted; (b) simplified representation of staggered 2D sheets along the [010] direction with nodes depicted as spheres. Hydrogen atoms and counter anions are omitted for clarity (symmetry codes $i = -1 + x, +y, +z$; $ii = +x, +y, -1 + z$); selected length (Å) and angles ($^\circ$) are reported in Table S5 in the SI.

Table 1
Dimensionality and nuclearity of silver(I) compounds obtained by using the nitrile functionalized pendant arm derivatives L¹-L¹².

Ligand	Silver(I) compound	Dimensionality and nuclearity	Schematic representation ^b	Ref.
L ¹	{[Ag(L ¹)](BF ₄)} _∞ ^a	3D		[13,14]
L ²	{[Ag(L ²)](BF ₄)} _∞	1D		[14]
L ³	{[Ag ₂ (L ³)](PF ₆) ₂ } _∞	2D		[14]
L ⁴	[Ag(L ⁴) ₂](BF ₄)	mononuclear	Sandwich complex	[17]
L ⁵	[Ag ₂ (L ⁵) ₂](BF ₄) ₂	binuclear		[14]
L ⁶	{[Ag(L ⁶)](BF ₄)} _∞	1D		[14]
L ⁷	[Ag ₂ (L ⁷) ₂](BF ₄) ₂	binuclear		[14]
L ⁸	{[Ag(L ⁸)](BF ₄)} _∞	1D		[14]
L ⁹	[Ag(L ⁹)](PF ₂ O ₂)	mononuclear	PF ₂ O ₂ ⁻ coordinates to silver(I) ^c	[14]
L ¹⁰	{[Ag(L ¹⁰)](BF ₄)} _∞	1D		This work
L ¹¹	{[Ag(L ¹¹)](BF ₄)} _∞	1D		This work
L ¹²	{[Ag(L ¹²)](NO ₃)} _∞	2D		This work

^a The same compound with the same structural features is obtained starting from AgPF₆ [14]; ^b black dots represent the silver(I) atoms in the schematic representations of the dimensionality and nuclearity of the compounds; linkers represent either N-(CH₂)_n-CN bridges (n = 1 L¹ and L⁸; n = 2 L², L³, L⁵, L⁶, L⁷), which can be single or double, or N-(CH₂)₃-N bridges (L¹²); in the case of L¹⁰ and L¹¹ a single S-donor bridges two metal centers; ^c PF₂O₂⁻ resulted from the hydrolysis of PF₆⁻ [14].

a crucial role [15,17]. In fact longer, more sterically-demanding nitrile-functionalized pendant arms of small tridentate macrocycles (L) do not appear to prevent CN⁻ or SCN⁻ forming a side-on two-electron (σ) bridge rather than a linear four-electron (σ + π) bridge between two [Ag(L)]⁺ units, independent of the nature of the counter-anion in the starting silver(I) metal salt (see Supporting Information for the structure of [Ag₂(L⁴)₂(μ-CN)](OTf)•½MeCN).

The results obtained with nitrile-functionalized pendant arm derivatives of larger 12-membered mixed-donor macrocycles such as L⁷ [14], L¹⁰, and L¹¹ indicate that in the formation of CPs with silver(I) the electronic requirements of the metal center and the coordination properties of the macrocyclic moiety and its donor set might become determinant.

In fact, despite the presence of the nitrile group in L¹⁰ and L¹¹, the metal ion prefers to catenate *via* a sulfur atom from the macrocycle unit bridging two metal ions in the formation of coordination polymers, and this seems to be a constant in the chemistry of functionalized derivatives of [12]aneNS₃ and [12]anePyNS₂ and is unaffected by the nature of the functional groups present in the pendant arm [24–26]. The results obtained with L¹² indicate that nitrile-functional groups implemented on open-chain ligand moieties such as Pypn can be a useful tool in determining the dimensionality of the resulting coordination polymers obtainable with silver (I), as demonstrated with simple aliphatic linear chain dinitriles NC(CH₂)_nCN [9–11].

4. Experimental

4.1. Materials and methods

The syntheses of the ligands L¹⁰-L¹² were carried out under N₂ atmosphere. L¹⁰ and L¹² were prepared according to procedures reported in refs. [18,19], respectively. The *N,N'*-bis(2-pyridylmethyl)-propylene-diamine (Pypn) precursor of L¹² was synthesized following the procedure reported in the literature for the preparation of its dimethylated derivative [38]. Reagents and solvents were used as purchased from Aldrich. Elemental analyses were performed with an EA1108 CHNS-O Fisons instrument (*T* = 1000 °C). ¹H NMR and ¹³C NMR spectra were determined on a Bruker Avance 600 MHz or a Varian INOVA-400 MHz spectrometers. Mass spectra were recorded on a triple quadrupole QQQ Varian 310-MS mass spectrometer by using the atmospheric pressure ESI technique. All the sample solutions were infused into the ESI source with a programmable syringe pump (1.50 mL/h constant flow rate). A dwell time of 14 s was used, and the spectra were accumulated for at least 10 min to increase the signal-to-noise ratio. Mass spectra were recorded in the *m/z* 100–1000 range.

Scan parameters were chosen to reduce/observe the fragmentation of the metal complexes [39]: needle voltage 3500 V, shield 800 V, source temperature 60 °C, drying gas pressure 20 psi, nebulizing gas pressure 20 psi, detector voltage 1450 V, and drying gas temperature 110 °C. The

isotopic patterns of the measured peaks in the mass spectra were analyzed using the mMass 5.5.0 software package [40]. All the mass values are indicated as monoisotopic masses, computed as the sum of the masses of the primary isotope of each atom in the molecule (note that the monoisotopic mass may differ from the nominal molecular mass).

4.2. X-ray diffraction

A summary of the crystal data and refinement details for the compounds discussed in this paper are given in Table S1 in the Supporting Information, only special features are noted here. X-ray diffraction data for $\{[Ag(L^{10})](BF_4)]_\infty$ and $\{[Ag(L^{11})](BF_4)\cdot\frac{1}{2}MeCN\}_\infty$ were collected at 100 K on a Bruker D8 Venture diffractometer (Mo $K\alpha$) equipped with a PHOTON II area detector. The data were indexed and processed using Bruker SAINT [41] and SADABS [42]. The structures were solved with the ShelXT 2018 [43] solution program using dual-space methods.

X-ray diffraction data for L^{10} , $\{[Ag(L^{12})](NO_3)]_\infty$ and $[Ag_2(L^4)_2(\mu-CN)](OTf)\cdot\frac{1}{2}MeCN$ were collected at 150 K on a Bruker SMART1000 diffractometer (Mo $K\alpha$) equipped with a CCD area detector. The data were indexed and processed using Bruker SAINT and SHELXTL [44]. The structures were solved with the ShelXS97 [45] structure solution program using direct methods.

The models were refined with ShelXL 2018 [46] using full-matrix least-squares minimization on F^2 . All non-hydrogen atoms were refined anisotropically. Hydrogen atom positions were calculated geometrically and refined using the riding model. Olex2 1.5 [47] was used as the graphical interface.

For L^{10} , during structure refinement, a portion of the macrocyclic unit (C7–C10, C12) was found to be affected by disorder; the disorder was modelled over two positions with fractional occupancies 81:19 by using geometrical restraints. For $\{[Ag(L^{11})](BF_4)\cdot\frac{1}{2}MeCN\}_\infty$, the co-crystallized acetonitrile molecule lies on a two-fold screw axis. Its methyl protons were, therefore, placed on calculated positions and their occupancies fixed to 0.5. Structures have been deposited with the Cambridge Crystallographic Data Centre via <https://www.ccdc.cam.ac.uk/deposit>, with deposition numbers CCDC: 2241473–2241477 for L^{10} , $[Ag_2(L^4)_2(\mu-CN)](OTf)\cdot\frac{1}{2}MeCN$, $\{[Ag(L^{12})](NO_3)]_\infty$, $\{[Ag(L^{10})](BF_4)]_\infty$, and $\{[Ag(L^{11})](BF_4)\cdot\frac{1}{2}MeCN\}_\infty$, respectively.

4.3. Synthesis of *N,N'*-bis(2-cyanoethyl)-*N,N'*-bis(2-pyridylmethyl)-propylenediamine (L^{12})

A mixture of *N,N'*-bis(2-pyridylmethyl)-propylenediamine (1.03 g, 5.05 mmol) and acrylonitrile (12 mL, 180 mmol) was stirred under N_2 atmosphere at 65 °C for 24 h. The excess of acrylonitrile was removed under vacuum to afford the desired compounds as a brownish oil in 90% yield. 1H NMR ($CDCl_3$, 400 MHz): δ_H 1.66 (t, $J = 6.8$ Hz, 2H), 2.42 (t, $J = 6.8$ Hz, 4H), 2.57 (t, $J = 6.8$ Hz, 4H), 2.77 (t, $J = 6.4$ Hz, 4H), 3.71 (s, 4H), 7.12 (t, $J = 7.2$ Hz, 2H), 7.41 (d, $J = 8.0$ Hz, 2H), 7.61 (t, $J = 7.6$ Hz, 2H), 8.45 (d, $J = 8.0$ Hz, 2H) ppm. ^{13}C NMR ($CDCl_3$, 100 MHz): δ_C 16.28, 25.02, 49.59, 51.75, 59.89, 118.96, 122.16, 122.95, 136.57, 148.85, 158.89 ppm. ESI(+)-MS (MeCN solution) m/z : 256 for $[L^{11}]^+$ ($[C_{15}H_{20}N_4]^+$).

4.4. Synthesis of $\{[Ag(L^{10})](BF_4)]_\infty$

$AgBF_4$ (0.016 g, 0.082 mmol) was added to a MeCN solution (10 mL) of L^{10} (5-(2-cyanoethyl)-2,8-dithia-5-aza-2,6-pyridinophane) (0.024 g, 0.082 mmol). The resulting colorless solution was stirred at room temperature under N_2 for 2 h in the dark. Diffusion of Et_2O vapors into the reaction mixture yielded colorless crystals of the CP $\{[Ag(L^{10})](BF_4)]_\infty$ (0.025 mg, 0.052 mmol, 63% yield). M.p.: 185 °C. Elemental Analysis (%) calcd. for $C_{14}H_{19}AgBF_4N_3S_2$: C 34.45, H 3.92, N 8.61, S 13.14. Found: C 34.40, H 3.96, N 8.58, S 13.19. 1H NMR (CD_3CN , 600 MHz): δ_H 2.43–2.45 (m, 2H), 2.52 (t, $J = 6.0$ Hz, 2H), 2.83 (t, $J = 6.0$ Hz, 2H), 2.90–2.93 (m, 2H), 3.28 (s, 4H), 3.80–4.20 (m, 4H), 7.30 (d, $J = 6.0$ Hz,

2H), 7.77 (t, $J = 6.0$ Hz, 1H) ppm. ^{13}C NMR ($CD_3CN/DMSO-d_6$, 150 MHz): δ_C 14.7, 30.4, 39.1, 48.4, 49.8, 52.0, 125.3, 139.5, 156.6 ppm. ESI (+)-MS (MeCN solution) m/z : 400 for $[L^{10}Ag]^+$ ($[C_{14}H_{19}Ag N_3S_2]^+$).

4.5. Synthesis of $\{[Ag(L^{11})](BF_4)\cdot\frac{1}{2}MeCN\}_\infty$

$AgBF_4$ (0.0414 g, 0.0246 mmol) was added to a MeCN solution (10 mL) of L^{11} (1-(2-cyanoethyl)-1-aza-4,7,10-trithiacyclododecane) (0.020 g, 0.072 mmol). The resulting colorless solution was stirred at room temperature under N_2 for 2 h in the dark. Diffusion of Et_2O vapors into the reaction mixture yielded colorless crystals (0.047 mg, 0.048 mmol, 66% yield). M.p.: 217 °C with decomposition. Elemental Analysis (%) calcd. for $C_{12}H_{21.5}AgBF_4N_{2.5}S_3$: C 29.31, H 4.41, N 7.12, S 19.57. Found: C 29.25, H 4.38, N 7.15, S 19.60. 1H NMR (CD_3CN , 600 MHz): δ_H 1.07 (t, $J = 6$ Hz, 1H), 1.90–1.93 (m, 1H), 2.40–2.45 (m, 1H), 2.59 (t, $J = 6$ Hz, 2H), 2.75–2.95 (m, 14H), 3.37 (q, $J = 6$ Hz, 1H) ppm. ^{13}C NMR ($CD_3CN/DMSO-d_6$, 150 MHz): δ_C 14.2, 15.5, 29.2, 29.5, 29.8, 49.4, 49.7, 66.0, 120.1 ppm. ESI(+)-MS (MeCN solution) m/z : 855 for $[Ag_2(L^{11})_2(BF_4)]^+$ ($[C_{22}H_{40}Ag_2BF_4N_4S_6]^+$).

4.6. Synthesis of $\{[Ag(L^{12})](NO_3)]_\infty$

$AgNO_3$ (0.033 g, 0.194 mmol) was added to a MeCN solution (10 mL) of L^{12} (*N,N'*-bis(2-cyanoethyl)-*N,N'*-bis(2-pyridylmethyl)-propylenediamine) (0.0721 g, 0.199 mmol). The resulting colorless solution was stirred at room temperature under N_2 for 2 h in the dark. Diffusion of Et_2O vapors into the reaction mixture yielded colorless crystals (0.025 g, 0.047 mmol, 24% yield). M.p.: 220 °C with decomposition. Elemental Analysis (%) calcd. for $C_{21}H_{26}AgN_7O_3$: C 47.38, H 4.92, N 18.42. Found: C 47.35, H 4.93, N 18.48. 1H NMR (CD_3CN , 600 MHz): δ_H 1.90 (m, 2H), 2.55 (m, 4H), 2.69 (m, 4H), 2.82 (m, 4H), 3.82 (s, 4H), 7.47 (m, 4H), 7.95 (m, 2H), 8.71 (d, $J = 5.4$ Hz, 2H). ^{13}C NMR (150 MHz, CD_3CN): δ_C 15.9, 24.3, 50.9, 56.0, 61.0, 119.9, 125.0, 126.4, 140.1, 152.5, 157.9. ESI(+)-MS (MeCN solution) m/z : 471 for $[L^{12}Ag]^+$ ($[C_{21}H_{26}AgN_6]^+$).

Declaration of Competing Interest

The authors declare that they have no known competing financial interests or personal relationships that could have appeared to influence the work reported in this paper.

Data availability

No data was used for the research described in the article.

Acknowledgments

The authors thank the Università degli Studi di Cagliari for financial support.

No data was used for the research described in this article.

Appendix A. Supplementary data

Supplementary data to this article can be found online at <https://doi.org/10.1016/j.ica.2023.121648>.

References

- [1] S. Wuttke, Introduction to reticular chemistry, *Angew. Chem. Int. Ed.* 58 (40) (2019) 14024.
- [2] H. Furukawa, K.E. Cordova, M. O'Keeffe, O.M. Yaghi, O'Keeffe, et al., The chemistry and applications of metal-organic frameworks, *Science* 341 (6149) (2013).
- [3] W.L. Leong, J.J. Vittal, One-dimensional coordination polymers: complexity and diversity in structures, properties, and applications, *Chem. Rev.* 111 (2) (2011) 688–764.

- [4] H. Li, L. Li, R.B. Lin, W. Zhou, Z. Zhang, S. Xiang, B. Chen, Porous metal-organic frameworks for gas storage and separation: status and challenges, *EnergyChem* 1 (2019), 100006.
- [5] N. Xia, Y. Chang, Q. Zhou, S. Ding, F. Gao, An overview of the design of metal-organic frameworks-based fluorescent chemosensors and biosensors, *Biosensors* 12 (2022) 928.
- [6] H.D. Lawesson, S.P. Walton, C. Chan, Metal-organic frameworks for drug delivery: a design perspective, *ACS Appl. Mater. Interf.* 13 (6) (2022) 7004–7020.
- [7] L.R. Mingabudinova, V.V. Vinogradov, V.A. Milichko, E. Hey-Hawkins, A. V. Vinogradov, Metal-organic frameworks as competitive materials for non-linear optics, *Chem. Soc. Rev.* 45 (19) (2016) 5408–5431.
- [8] **Advanced Structural Chemistry: Tailor Made, Properties and Applications of Inorganic Materials (Vol. 2)**, R. Cao (Ed), WILEY-VCH GmbH (2021) ISBN: 9783527349005.
- [9] L. Carlucci, G. Ciani, D.M. Proserpio, S. Rizzato, Coordination networks from the self-assembly of silver salts and the linear chain dinitriles $\text{NC}(\text{CH}_2)_n\text{CN}$ ($n = 2$ to 7): a systematic investigation of the role of counterions and of the increasing length of the spacers, *CrstEngComm* 4 (70) (2002) 413–425.
- [10] L. Carlucci, G. Ciani, P. Macchi, D.M. Proserpio, S. Rizzato, Complex interwoven polymeric frames from the self-assembly of silver(I) cations and sebaconitrile, *Chem. Eur. J.* 5 (1) (1999) 237–243.
- [11] L. Carlucci, G. Ciani, M.D. Proserpio, S. Rizzato, Three novel interpenetrating diamantoid networks from self-assembly of 1,12-dodecanedinitrile with silver(I) salts, *Chem. Eur. J.* 8 (7) (2002) 1519–1526.
- [12] A.N. Khloubstov, A.J. Blake, N.R. Champness, D.A. Lemenovskii, A.G. Majouga, N. V. Zyk, M. Schröder, Supramolecular design of one-dimensional coordination polymers based on silver(I) complexes of aromatic nitrogen-donor ligands, *Coord. Chem. Rev.* 222 (1) (2001) 155–192.
- [13] L. Tei, V. Lippolis, A.J. Blake, P.A. Cooke, M. Schröder, Nitrile functionalized pendant-arm derivatives of [9]aneN₃ as a new multidentate ligands for inorganic crystal engineering ([9]aneN₃ = 1,4,7-triazacyclononane), *Chem. Commun.* (1998) 2633–2634.
- [14] L. Tei, A.J. Blake, P.A. Cooke, C. Caltagirone, F. Demartin, V. Lippolis, F. Morale, C. Wilson, M. Schröder, Nitrile functionalized pendant-arm derivatives of aza- and mixed donor macrocyclic ligands as new building blocks for inorganic crystal engineering, *J. Chem. Soc. Dalton Trans.* (2002) 1662–1670.
- [15] V. Lippolis, A.J. Blake, P.A. Cooke, F. Isaia, W.S. Li, M. Schröder, Synthesis and full characterization of the first discrete binuclear complex featuring a two-electron (σ) μ_2 -kC:kC bridging cyanide, *Chem. Eur. J.* 5 (1999) 1987–1991.
- [16] A.J. Blake, J.P. Danks, V. Lippolis, S. Parsons, M. Schröder, Self-assembly of a polynuclear ribbon: the structure of $\{[\text{Cu}_2(\text{CN})_2(\text{L})] \cdot \text{MeNO}_2\}_\infty$ [L = 4,7-bis(2-cyanoethyl)-1-thia-4,7-diazacyclononane], *New J. Chem.* 22 (1998) 1301–1303.
- [17] A.J. Blake, V. Lippolis, M. Schröder, Coordination chemistry of nitrile-functionalized mixed thia-aza macrocycles [9]aneN₂S and [9]aneNS₂ towards silver(I), *Acta Cryst. C* 78 (2022) 169–175.
- [18] A.J. Blake, A. Bencini, C. Caltagirone, G. De Filippo, L.S. Dolci, A. Garau, F. Isaia, V. Lippolis, P. Mariani, L. Prodi, M. Montalti, N. Zaccheroni, C. Wilson, A new pyridine-based 12-membered macrocycle functionalised with different fluorescent subunits; coordination chemistry towards Cu^{II}, Zn^{II}, Cd^{II}, Hg^{II}, and Pb^{II}, *Dalton Trans.* (17) (2004) 2771–2779.
- [19] M.C. Aragoni, M. Arca, A. Bencini, A.J. Blake, C. Caltagirone, A. Decortes, F. Demartin, F.A. Devillanova, E. Faggi, L.S. Dolci, A. Garau, F. Isaia, V. Lippolis, L. Prodi, C. Wilson, B. Valtancoli, N. Zaccheroni, Coordination chemistry of *N*-aminopropyl pendant arm derivatives of mixed N/S, and N/S/O-donor macrocycles, and construction of selective fluorimetric chemosensors for heavy metal ions, *Dalton Trans.* (18) (2005) 2994.
- [20] J.P. Danks, N.R. Champness, M. Schröder, Chemistry of mixed nitrogen- and sulfur-donor tridentate macrocycles, *Coord. Chem. Rev.* 174 (1) (1998) 417–468.
- [21] O.K. Rasheed, C. Bawn, D. Davies, J. Raftery, I. Victorica-Yrzebal, R. Pritchard, H. Zhou, P. Quayle, The Synthesis of group 10 and 11 metal complexes of 3,6,9-trithia-1-(2,6)-pyridinacyclodecaphane and their use in A³-coupling reactions, *Eur. J. Org. Chem.* 35 (2017) 5252–5261.
- [22] P.J. Reddy, V. Ravichandran, K.K. Chacko, E. Weber, W. Saenger, Structure of the 2,5,8-trithia[9](2,6)pyridinophane-silver nitrate complex (1:1), *Acta Cryst. C* 45 (12) (1989) 1871–1874.
- [23] Y. Habata, F. Osaka, Dimetallo[3.3]para- and metacyclophanes by self-assembly of pyridylmethyl armed-monoazatrithia- and monoazadithiaoxa-12-crown-4 ethers with Ag⁺, *Dalton Trans.* (2006) 1836–1841.
- [24] Y. Habata, K. Noto, F. Osaka, Substituents effects on the structures of silver complexes with monoazatrithia-12-crown-4 ethers bearing substituted aromatic rings, *Inorg. Chem.* 46 (2007) 6529–6534.
- [25] J.B. Love, J.M. Vere, M.W. Glenny, A.J. Blake, M. Schröder, Ditopic azathioether macrocycles as hosts for transition metal salts, *Chem. Commun.* (2001) 2678–2679.
- [26] M.W. Glenny, M. Lacombe, J.B. Love, A.J. Blake, L.F. Lindoy, R.C. Luckay, K. Gloe, B. Antoniolli, C. Wilson, M. Schröder, Design and synthesis of heteroditopic azathioether macrocycles for metal extraction, *New J. Chem.* 30 (2006) 1755–1767.
- [27] E. Podda, S.J. Coles, P.N. Horton, P.D. Lickis, O.S. Bull, J.B. Orton, A. Pintus, D. Pugh, M.C. Aragoni, R.P. Davies, First example of solid-state luminescence borasiloxane-based chiral helices assembled through N-B bonds, *Dalton Trans.* 50 (2021) 3782–3785.
- [28] A. Mohamadou, G.A. van Albada, I. Mitkainen, U. Turpeinen, J. Marrot, J. Reedijk, Synthesis, crystal structure, hydrogen bonding and spectroscopy of transition-metal complexes with the ligand (N, N'-bis(2-pyridylmethyl)-1,3-propanediamine), *Polyhedron* 28 (2009) 2813–2820.
- [29] E.D. McKenzie, F.S. Stephens, Metal compounds of tetra-amines with terminal pyridyl residues. Crystal and molecular structures of $[\text{M}(\text{C}_{15}\text{H}_{20}\text{N}_4)](\text{ClO}_4)_2$ (M = Pd, Cu), *Inorg. Chim. Acta* 42 (1980) 1–10.
- [30] A. Mohamadou, G.A. van Albada, I. Mitkainen, U. Turpeinen, J. Marrot, J. Reedijk, Synthesis, crystal structure, hydrogen bonding and spectroscopy of Co³⁺, Mn³⁺, and Ni²⁺ oxalate complexes with the ligand (N, N'-bis(2-pyridylmethyl)-1,3-propanediamine), *Inorg. Chim. Acta* 363 (2010) 3023–3027.
- [31] M. Ardon, A. Bino, K. Michelsen, E. Pedersen, Long-distance magnetic exchange between chromium(III) atoms bridged by H₃O₂ ligands, *J. Am. Chem. Soc.* 109 (19) (1987) 5855–5856.
- [32] N. Shaikh, S. Goswami, A. Panja, H.L. Sun, F. Pan, S. Gao, P. Banerjee, Syntheses, crystal structures, and spectroscopic and magnetic properties of $[\text{Mn}_2^{\text{III}}(\text{H}_2\text{L})^+ (\text{Cl}_4\text{Cat})_4 \cdot 2\text{H}_2\text{O}]_\infty$ and $[\text{Mn}_2^{\text{III}}(\text{H}_2\text{L}^2)(\text{Cl}_4\text{Cat})_4 \cdot 2\text{CH}_3\text{CN} \cdot 2\text{H}_2\text{O}]_\infty$: temperature-dependent valence tautomerism in solution, *Inorg. Chem.* 44 (2005) 9714–9722.
- [33] D.J. Hodgson, K. Michelsen, E. Pedersen, D.K. Towle, Tetranuclear heterometallic complexes of the general types $[\text{M}(\text{OH})_2\text{CrA}_4]_3^{5+}$ and $[\text{M}(\text{OH})_2\text{CoA}_4]_3^{5+}$, *Inorg. Chem.* 30 (4) (1991) 815–822.
- [34] P.A. Goodson, J. Glerup, D.J. Hodgson, K. Michelsen, H. Weihe, Syntheses and characterization of binuclear manganese (III, IV) and -(IV, IV) complexes with ligands related to N, N'-bis(2-pyridylmethyl)-1,2-ethanediamine, *Inorg. Chem.* 30 (1991) 4909–4914.
- [35] R. Montis, M.C. Aragoni, C. Bazzicalupi, A.J. Blake, C. Caltagirone, G. De Filippo, A. Garau, P. Gratteri, F. Isaia, V. Lippolis, A. Pintus, Bis(2-pyridylmethyl)alkyl (thioalkyl)diamine as promising scaffolds for the construction of fluorescent and redox chemosensors for transition metal ions, *Inorg. Chim. Acta* 381 (2012) 170–180.
- [36] M. Shamsipur, A. Taherpour, V. Lippolis, R. Montis, Development of a novel PVC-membrane fluorescent sensor based on N, N'-bis(dansylamidoethyl)-N, N'-bis(2-pyridylmethyl)propylenediamine as a new fluoroionophore for highly sensitive and selective monitoring of trace amounts of La³⁺ ions in aqueous solutions, *Sens. Actuators B: Chemical* 192 (2014) 378–385.
- [37] J. Huang, Z.P. Deng, Y.H. Xiao, L.H. Huo, S.N. Zhao, F.Y. Ge, S. Gao, Macrocyclic dinuclear, helical, layered and 3-D Ag(I) complexes constructed from AgX (X = NO₃⁻ and ClO₄⁻) and flexible bis(pyridyl) ligands with a chelating spacer: syntheses, structures and photoluminescence properties, *Dalton Trans.* 44 (2015) 5837–5847.
- [38] C.-M. Che, W.-T. Tang, C.-K. Li, Synthesis, electrochemistry, and reactivities of *trans*-[Ru^{VI}(L)O₂]²⁺ (L = N, N'-dimethyl-N, N'-bis(2-pyridylmethyl)propylenediamine), *J. Chem. Soc., Dalton Trans.* (12) (1990) 3735–3739.
- [39] S. Masuri, E. Cadoni, M.G. Cabiddu, F. Isaia, M.G. Demuru, L. Morañ, D. Buček, P. Vaňhara, J. Havel, T. Pivetta, The first copper(II) complex with 1,10-phenanthroline and salubrinol with interesting biochemical properties, *Metallomics* 12 (2020) 891–901.
- [40] M. Strohm, D. Kavan, P. Novak, M. Volný, V. Havlíček, mMass 3: cross-platform software environment for precise analysis of mass spectrometric data, *Anal. Chem.* 82 (2010) 4648–4651.
- [41] SAINT Version 8.37 A; Bruker AXS Inc.: Wisconsin (USA), (2013).
- [42] SADABS Version 2016/2; Bruker AXS Inc.: Wisconsin (USA), (2016).
- [43] G.M. Sheldrick, SHELXT – integrated space-group and crystal-structure determination, *Acta Cryst. A* 71 (1) (2015) 3–8, <https://doi.org/10.1107/S2053273314026370>.
- [44] SHELXTL; Bruker AXS Inc.: Wisconsin (USA), (2001).
- [45] G.M. Sheldrick, A short history of ShelX, *Acta Cryst. A* 64 (2008) 112–122, <https://doi.org/10.1107/S0108767307043930>.
- [46] G.M. Sheldrick, Crystal structure refinement with SHELXL, *Acta Cryst. C* 71 (1) (2015) 3–8, <https://doi.org/10.1107/S2053229614024218>.
- [47] O.V. Dolomanov, L.J. Bourhis, R.J. Gildea, J.A.K. Howard, H. Puschmann, OLEX2: A complete structure solution, refinement and analysis program, *J. Appl. Cryst.* 42 (2009) 339–341, <https://doi.org/10.1107/S0021889808042726>.